

Constraining Star-Formation Driven Outflows in Local Dwarf Galaxies with *Herschel*[†]

Michael Romano^{1,2,*} ¹ National Centre for Nuclear Research, ul. Pasteura 7, 02-093 Warsaw, Poland² INAF - Osservatorio Astronomico di Padova, Vicolo dell'Osservatorio 5, I-35122, Padova, Italy

* Correspondence: michael.romano@ncbj.gov.pl

[†] Presented at the 2nd Electronic Conference on Universe, 16 February–2 March 2023; Available online:<https://ecu2023.sciforum.net/>.

Abstract: Galactic feedback (i.e., outflows) plays a fundamental role in regulating galaxy formation and evolution. We investigate the physical properties of galactic outflows in a sample of 29 local low-metallicity dwarf galaxies drawn from the Dwarf Galaxy Survey. We make use of *Herschel*/PACS archival data to detect outflows in the broad wings of observed [CII] 158 μm line profiles. We detect outflowing gas in 1/3 of the sample, and in the average galaxy population through line stacking. We find typical mass-loading factors (i.e., outflow efficiencies) of the order of unity. Outflow velocities are larger than the velocities required from gas to escape the gravitational potential of our targets, suggesting that a significant amount of gas and dust is brought out of their halos. Our results will be used as input for chemical models, posing new constraints on the processes of dust production/destruction in the interstellar medium of galaxies.

Keywords: Galaxies: dwarf; Galaxies: evolution; Galaxies: ISM; Galaxies: starburst; ISM: jet and outflows

1. Introduction

Galactic winds can originate both from stellar processes and active galactic nuclei (AGNs), being of key importance in regulating the formation and evolution of their host galaxies across cosmic time. Nearby dwarf galaxies are very sensitive to such feedback, thus representing the perfect target for a detailed investigation of galactic outflows and their impact on galaxy evolution. One of the most widespread techniques used to characterize outflows at different redshifts consists in decomposing emission line profiles into a narrow and broad Gaussian components, which are supposed to trace the virial motion of stars in the galaxies and the outflowing gas, respectively. This method has been successfully applied to the [CII] line at 158 μm rest-frame, one of the strongest fine-structure lines in the far-infrared (FIR) spectra of star-forming galaxies (SFGs; e.g., [1]), resulting in the detection of high-velocity outflows in high- z luminous quasars, and in *normal* SFGs at $z > 4$ via stacking [2,3] thanks to IRAM and ALMA observations, respectively. *Herschel* data have been used to trace atomic (and possibly molecular) outflows in the broad [CII] wings of local ultra-luminous infrared galaxies (ULIRGs; [4]), as well.

We here investigate the importance of stellar feedback in the evolution of galaxies by constraining the efficiency of galactic outflows in local dwarf sources. We make use of archival spectroscopic [CII] observations as collected by *Herschel*/PACS in the sample of local dwarf galaxies drawn from the Dwarf Galaxy Survey (DGS; [5]). We derive the physical properties of outflows in these sources, in order to characterize their origin, efficiency, and impact on the interstellar medium (ISM) and environment of their host galaxies. Our results are suitable for tuning state-of-the-art chemical evolution models (e.g., [6]) which attempt to reproduce the processes shaping the evolution of galaxies across cosmic times.



Citation: Romano, M. Galactic outflows in local dwarf galaxies. *Phys. Sci. Forum* **2023**, *1*, 0. <https://doi.org/>

Published: 23 February 2023



Copyright: © 2023 by the authors. Licensee MDPI, Basel, Switzerland. This article is an open access article distributed under the terms and conditions of the Creative Commons Attribution (CC BY) license (<https://creativecommons.org/licenses/by/4.0/>).

Throughout this work, we adopt a Λ -CDM cosmology with $H_0 = 70 \text{ km s}^{-1} \text{ Mpc}^{-1}$, $\Omega_m = 0.3$ and $\Omega_\Lambda = 0.7$. Section 2 presents the data and the methods used to identify galactic outflows. In Section 3 we discuss the major results obtained. Summary and conclusions are reported in Section 4.

2. Methods

The DGS survey undertake *Herschel* observations of 48 low-metallicity dwarf galaxies ($\log(M_*/M_\odot) \sim 6 - 10$) in the local Universe ($D \lesssim 200 \text{ Mpc}$). The original sample is composed of 37 compact objects and 11 extended sources. The latter were excluded from this analysis as they were covered only partially by the PACS spectrograph. Moreover, two other sources were dropped from the PACS spectroscopy program because of time constraints [7]. We thus downloaded *Herschel* archival data cubes of [CII] emission for the resulting 35 galaxies. We used the *Herschel* Interactive Processing Environment (HIPE; [8]), version 15.0.1, on the cubes to extract the best spectrum (with the largest flux and a highest signal-to-noise) for each source. We further avoided 6 objects because their [CII] spectra were too noisy to be analyzed, ending up with a final sample of 29 galaxies. We examined the continuum-subtracted spectrum of each of these sources by fitting it with a single and double Gaussian profile (including in the latter a narrow and broad component), and by looking for an excess of emission in the high-velocity tails of the corresponding residuals. We compared the reduced χ^2 of the fit with the single (χ_{single}^2) and double (χ_{double}^2) Gaussian profiles, considering the presence of the possible outflow component only when $\chi_{\text{double}}^2 < \chi_{\text{single}}^2$. We found that 11 out of 29 galaxies show clear signs of outflowing gas as traced by the [CII] emission, while in the remaining sources the outflow (if present) is too faint to be individually detected. The physical parameters of the sources in our sample were retrieved by fitting their spectral energy distributions with the Code Investigating GALaxy Emission (CIGALE; [9–11]), **which placed them (within the uncertainties) along the main-sequence of star-forming galaxies (e.g., [12]) in the local universe.**

2.1. Individual and average outflow properties

The 11 galaxies with individual outflow detections show a significant residual emission at velocities of $\pm 400 \text{ km s}^{-1}$ when modeling their [CII] spectra with a single Gaussian component. These residuals can be reduced to the noise level by adding a broad component to the fit, thus highlighting the presence of outflowing gas. We computed the [CII] luminosity of both components by following [13], as

$$L_{[\text{CII}]} = 1.04 \times 10^{-3} S_{[\text{CII}]} \Delta v D_L (z_{[\text{CII}]})^2 \nu_{\text{obs}} [L_\odot], \quad (1)$$

where $S_{[\text{CII}]} \Delta v$ is the velocity-integrated line flux in units of Jy km s^{-1} , ν_{obs} is the observed peak frequency in Gigahertz, and D_L is the luminosity distance in Mpc at the redshift derived from the centroid of the single Gaussian fit of the [CII] line (i.e., $z_{[\text{CII}]}$).

To get the average outflow properties of our galaxy sample we performed a stacking of their [CII] spectra. First, we used the computed $z_{[\text{CII}]}$ to align each continuum-subtracted spectrum to the [CII] rest-frame frequency. Then, we proceeded with a variance-weighted stacking as

$$S_{\text{stack}} = \frac{\sum_{i=1}^N S_i \cdot w_i}{\sum_{i=1}^N w_i}, \quad (2)$$

where S_i is the [CII] spectrum of the i -th galaxy, N is the number of stacked sources, and $w_i = 1/\sigma_i^2$ is the weighting factor (with σ_i the noise associated to each spectrum). We show in Figure 1 (left panel) the result of this procedure. We again fitted the stacked spectrum with both a single and double Gaussian profile, comparing the corresponding reduced χ^2 and residuals. The spectrum shows clear signs of broad wings at velocities $\pm \sim 400 \text{ km s}^{-1}$ as evidenced by the corresponding large residuals obtained by using a single Gaussian function to fit the line profile. We also repeated the stacking by only including those

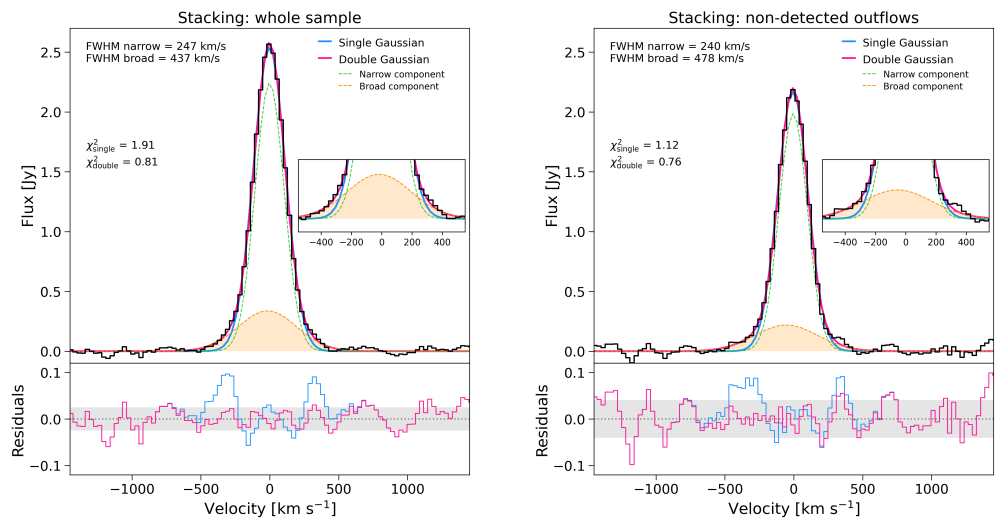


Figure 1. *Left:* Stacked variance-weighted [CII] spectrum (black histogram) of the whole sample as a function of velocity. The blue (pink) line represents the fit with a single (double) Gaussian function. The green and orange lines are the narrow and broad components of the double Gaussian, respectively. The FWHM of both components and the corresponding reduced χ^2 are also shown in the figure. A zoom-in of the spectral region dominated by outflows is shown as an inset plot on the right. The bottom panel reports the residuals from the single and double Gaussian functions. The dotted horizontal line marks the zero level, while the shaded area represents the noise of each spectrum at $\pm 1\sigma$. *Right:* same as left panel, but for the stacking of only the sources with non-detected outflows.

sources with no individual outflow detection. This latter stacking is displayed in Figure 1 (right panel), where the spectrum is still affected by broad wings in its high-velocity tails, although they appear weaker than those found by stacking the whole sample. Once more, for both spectra, we estimated the [CII] luminosity of the broad components through Equation 1.

Finally, we characterized the average spatial extent of the atomic outflows in our galaxies by spatially stacking their [CII] cubes. As done for the spectral stacking, we aligned the spectral axes of each continuum-subtracted cube to the [CII] rest-frame emission. Then, we also spatially aligned the cubes by centering them on the peak of the corresponding [CII] intensity map produced by summing the fluxes from the spectral channels including the emission line. We used a variance-weighted stacking as in Equation 2, where σ is now the spatial rms estimated in each channel of the cube in regions free of emission. We produced velocity-integrated [CII] maps of the wings at $[-500, -250]$ and $[250; 500]$ km s^{-1} , and added the two maps together to obtain the total outflow emission. We thus fitted a 2D Gaussian function to the total intensity map of the wings obtaining the outflow circularized effective radius as $R_{\text{out}} = \sqrt{ab}$, where a and b are the best-fit beam-deconvolved semi-major and semi-minor axis of the Gaussian, respectively. We found $R_{\text{out}} = 0.99 \pm 0.39$ kpc.

3. Results and Discussion

3.1. Outflow efficiency

A fundamental parameter for characterizing galactic outflows and their impact on the evolution of their host galaxies is the so-called mass-loading factor, i.e., the ratio between the rate of gas mass expelled out of the galaxy and the rate of star formation ($\eta = \dot{M}_{\text{out}}/\text{SFR}$). This quantity represents an estimate of the outflow efficiency and it is a key ingredient for simulations trying to explain the baryon cycle in galaxies. Following [14], we used the [CII] luminosity of the broad component (both for individual outflow detections and stacked

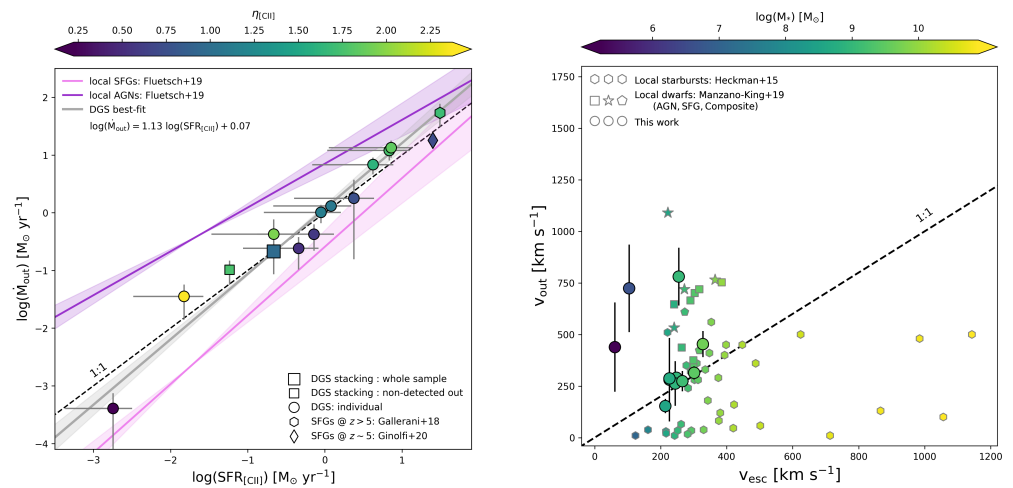


Figure 2. *Left:* Atomic outflow rate as a function of the SFR, for both individual detections of broad wings (circles) and from line stacking of the whole sample and of the sources with non-detected outflow (big and small squares, respectively). The pink and violet lines are the best-fit relations between molecular outflow rate and SFR for local AGN hosts and star-forming/starburst galaxies by [15], while the shaded regions are the corresponding uncertainties. The solid grey line with the shaded area represent a linear fit to the DGS galaxies with individual outflow detections and its uncertainty, respectively. The dashed line reports the 1:1 relation. We also show the results from [CII] stacking of $z \gtrsim 5$ SFGs by [16] (hexagon) and [3] (diamond). All markers are color-coded for their mass-loading factors. *Right:* Relation between the outflow velocity and the escape velocity. Galaxies of our sample with individual outflow detections are shown as circles. Local starbursts are represented by hexagons [17]. Nearby dwarf galaxies, including AGNs, star forming and composite galaxies, are shown as squares, stars, and pentagons, respectively [18]. The dashed line reports the 1:1 relation. All data are color-coded for their stellar mass.

spectra) to estimate the mass of the outflowing atomic gas, which is needed to compute the mass outflow rate as

$$\dot{M}_{\text{out}} = \frac{v_{\text{out}} \times M_{\text{out}}}{R_{\text{out}}}, \tag{3}$$

where $v_{\text{out}} = FWHM_{\text{broad}}/2 + |v_{\text{broad}} - v_{\text{narrow}}|$ is the outflow velocity (with $FWHM_{\text{broad}}$ the full width at half maximum of the broad component, while v_{broad} and v_{narrow} the velocity peaks of the broad and narrow components, respectively), and R_{out} is the outflow radius.

We show in Figure 2 (left panel) the atomic outflow rate as a function of the SFR as obtained from the spectral stacking of our galaxies and from individual detections of the broad component. We also report the best-fit relations between molecular outflow rate and SFR for both local AGNs and starburst/SFGs as found by [15]. Most of our galaxies lie along the 1:1 relation with an average mass-loading factor $\eta \sim 1.3$. However, we note that, if all the phases (atomic, ionized, molecular) of the ISM would contribute equally to the outflow rate (e.g., [15]), we could obtain an average outflow efficiency three times larger than estimated (i.e., $\eta \gtrsim 3$). From the stacking of the whole sample (of the galaxies with non-detected outflows) we found similar results, that is $\eta = 0.97$ ($\eta = 1.76$). By fitting the individual outflow detections we obtained $\log(\dot{M}_{\text{out}}) = 1.13 \log(\text{SFR}_{[\text{CII}]}) + 0.05$, with the slope in agreement with that found by [15] for local SFGs, although closer to the 1:1 relation. Furthermore, we compare our results to those found at high redshift by [16] and [3], who took advantage of [CII] emission detected in SFGs at $4 < z < 6$. Both results are in good agreement with our findings, suggesting that similar feedback mechanisms could be in place in this kind of galaxies.

3.2. Outflow escaping velocity

We computed the escape velocities (v_{esc}) needed by outflows to escape the gravitational potential of their host galaxies, as

$$v_{\text{esc}}(r) = \sqrt{2|\Phi(r)|} = \sqrt{\frac{2M_{\text{halo}}G}{r(\ln(1+c) - c/(1+c))} \ln(1+r/r_s)}, \quad (4)$$

where G is the gravitational constant, c is the concentration parameter, M_{halo} is the mass of the halo, and $r_s = r_{\text{halo}}/c$ is the characteristic radius, with r_{halo} as the virial radius. Here, the halo mass was obtained from the stellar mass of the corresponding galaxy through abundance matching techniques, while the virial radius is defined as

$$r_{\text{halo}} = \left[\frac{3M_{\text{halo}}}{4\pi \cdot 200 \rho_{\text{crit},0}} \right]^{1/3}, \quad (5)$$

with $\rho_{\text{crit},0}$ being the present critical density. In Figure 2 (right panel), we show the velocity of the outflow as a function of the escape velocity for each galaxy with individual outflow detection. As a comparison, we display the results by [17] for ionized outflows in a sample of ~ 40 local starbursts, and by [18] from Keck spectroscopy of local dwarf galaxies (including AGNs and SFGs). The most massive galaxies (i.e., $\log(M_*/M_\odot) \gtrsim 10$) lie below the 1:1 relation at large escape velocities, implying that outflows in these sources (at least from the ionized phase) are not able to expel material outside of their dark matter halos. On the contrary, all of our sources are close or above the relation, with outflow velocities higher than (or comparable to) the escape ones, in agreement with the results for local dwarf galaxies by [18]. This suggests that galactic outflows in these objects are able to bring material at least in their circumgalactic medium (CGM), having a significant impact on their baryon cycle.

4. Conclusions

In this paper, we investigate the impact of galactic outflows in the evolution of local low-metallicity dwarf galaxies drawn from the DGS survey. In particular, we take advantage of *Herschel* observations of their [CII] emission to study how galactic winds affect their hosts. We found clear evidence of outflowing gas in 1/3 of our sample, with an average mass-loading factor consistent with unity (although this could be three times larger if we account for the ionized and molecular ISM phases, which are not traced by the [CII] emission). We then estimated the escape velocities needed by outflows to bring the gas outside of the galaxies. We found that, for all our galaxies, outflows are fast enough to expel material into the CGM of their hosts, where the gas can be later re-accreted by galaxies as fuel for new star formation, or it can become unbound from their gravitational potential enriching the intergalactic medium. Our results could be used for tuning chemical evolution models trying to reproduce observational properties of both local and distant galaxies, thus providing a more robust characterization of the physical processes shaping their evolution across cosmic time. However, a more in-depth investigation is needed in order to provide a complete picture of feedback effect in local galaxies. Future observations will allow us to enlarge our current sample with ionized and molecular data, gaining a complete description of all the outflow phases affecting the ISM and external environment of galaxies.

Funding: This research was funded by Narodowe Centrum Nauki, grant number UMO-2020/38/E/ST9/00077.

Institutional Review Board Statement: Not applicable.

Informed Consent Statement: Not applicable.

Acknowledgments: HIPE is a joint development by the *Herschel* Science Ground Segment Consortium, consisting of ESA, the NASA *Herschel* Science Center, and the HIFI, PACS and SPIRE consortia. M.R. acknowledges support from the Narodowe Centrum Nauki (UMO-2020/38/E/ST9/00077).

Conflicts of Interest: The authors declare no conflict of interest.

References

1. Carilli, C.L.; Walter, F. Cool Gas in High-Redshift Galaxies. *ARA&A* **2013**, *51*, 105–161, [arXiv:astro-ph.CO/1301.0371]. <https://doi.org/10.1146/annurev-astro-082812-140953>.
2. Cicone, C.; Maiolino, R.; Gallerani, S.; Neri, R.; Ferrara, A.; Sturm, E.; Fiore, F.; Piconcelli, E.; Feruglio, C. Very extended cold gas, star formation and outflows in the halo of a bright quasar at $z > 6$. *A&A* **2015**, *574*, A14, [arXiv:astro-ph.GA/1409.4418]. <https://doi.org/10.1051/0004-6361/201424980>.
3. Ginolfi, M.; Jones, G.C.; Béthermin, M.; Fudamoto, Y.; Loiacono, F.; Fujimoto, S.; Le Fèvre, O.; Faisst, A.; Schaerer, D.; Cassata, P.; et al. The ALPINE-ALMA [C II] survey: Star-formation-driven outflows and circumgalactic enrichment in the early Universe. *A&A* **2020**, *633*, A90, [arXiv:astro-ph.GA/1910.04770]. <https://doi.org/10.1051/0004-6361/201936872>.
4. Janssen, A.W.; Christopher, N.; Sturm, E.; Veilleux, S.; Contursi, A.; González-Alfonso, E.; Fischer, J.; Davies, R.; Verma, A.; Graciá-Carpio, J.; et al. Broad [C II] Line Wings as Tracer of Molecular and Multi-phase Outflows in Infrared Bright Galaxies. *ApJ* **2016**, *822*, 43, [arXiv:astro-ph.GA/1604.00185]. <https://doi.org/10.3847/0004-637X/822/1/43>.
5. Madden, S.C.; Rémy-Ruyer, A.; Galametz, M.; Cormier, D.; Lebouteiller, V.; Galliano, F.; Hony, S.; Bendo, G.J.; Smith, M.W.L.; Pohlen, M.; et al. An Overview of the Dwarf Galaxy Survey. *Publ. Astron. Soc. Pac.* **2013**, *125*, 600, [arXiv:astro-ph.GA/1305.2628]. <https://doi.org/10.1086/671138>.
6. Nanni, A.; Burgarella, D.; Theulé, P.; Côté, B.; Hirashita, H. The gas, metal, and dust evolution in low-metallicity local and high-redshift galaxies. *A&A* **2020**, *641*, A168, [arXiv:astro-ph.GA/2006.15146]. <https://doi.org/10.1051/0004-6361/202037833>.
7. Cormier, D.; Madden, S.C.; Lebouteiller, V.; Abel, N.; Hony, S.; Galliano, F.; Rémy-Ruyer, A.; Bigiel, F.; Baes, M.; Boselli, A.; et al. The *Herschel* Dwarf Galaxy Survey. I. Properties of the low-metallicity ISM from PACS spectroscopy. *A&A* **2015**, *578*, A53, [arXiv:astro-ph.GA/1502.03131]. <https://doi.org/10.1051/0004-6361/201425207>.
8. Ott, S. The *Herschel* Data Processing System — HIPE and Pipelines — Up and Running Since the Start of the Mission. In Proceedings of the Astronomical Data Analysis Software and Systems XIX; Mizumoto, Y.; Morita, K.I.; Ohishi, M., Eds., 2010, Vol. 434, *Astronomical Society of the Pacific Conference Series*, p. 139, [arXiv:astro-ph.IM/1011.1209].
9. Burgarella, D.; Buat, V.; Iglesias-Páramo, J. Star formation and dust attenuation properties in galaxies from a statistical ultraviolet-to-far-infrared analysis. *MNRAS* **2005**, *360*, 1413–1425, [arXiv:astro-ph/astro-ph/0504434]. <https://doi.org/10.1111/j.1365-2966.2005.09131.x>.
10. Noll, S.; Burgarella, D.; Giovannoli, E.; Buat, V.; Marcellac, D.; Muñoz-Mateos, J.C. Analysis of galaxy spectral energy distributions from far-UV to far-IR with CIGALE: studying a SINGS test sample. *A&A* **2009**, *507*, 1793–1813, [arXiv:astro-ph.CO/0909.5439]. <https://doi.org/10.1051/0004-6361/200912497>.
11. Boquien, M.; Burgarella, D.; Roehlly, Y.; Buat, V.; Ciesla, L.; Corre, D.; Inoue, A.K.; Salas, H. CIGALE: a python Code Investigating GALaxy Emission. *A&A* **2019**, *622*, A103, [arXiv:astro-ph.GA/1811.03094]. <https://doi.org/10.1051/0004-6361/201834156>.
12. Rodighiero, G.; Daddi, E.; Baronchelli, I.; Cimatti, A.; Renzini, A.; Aussel, H.; Popesso, P.; Lutz, D.; Andreani, P.; Berta, S.; et al. The Lesser Role of Starbursts in Star Formation at $z = 2$. *ApJL* **2011**, *739*, L40, [arXiv:astro-ph.CO/1108.0933]. <https://doi.org/10.1088/2041-8205/739/2/L40>.
13. Solomon, P.M.; Downes, D.; Radford, S.J.E. Warm Molecular Gas in the Primeval Galaxy IRAS 10214+4724. *ApJL* **1992**, *398*, L29. <https://doi.org/10.1086/186569>.
14. Hailey-Dunsheath, S.; Nikola, T.; Stacey, G.J.; Oberst, T.E.; Parshley, S.C.; Benford, D.J.; Staguhn, J.G.; Tucker, C.E. Detection of the $158 \mu\text{m}$ [C II] Transition at $z = 1.3$: Evidence for a Galaxy-wide Starburst. *ApJL* **2010**, *714*, L162–L166, [arXiv:astro-ph.CO/1003.2174]. <https://doi.org/10.1088/2041-8205/714/1/L162>.
15. Fluetsch, A.; Maiolino, R.; Carniani, S.; Marconi, A.; Cicone, C.; Bourne, M.A.; Costa, T.; Fabian, A.C.; Ishibashi, W.; Venturi, G. Cold molecular outflows in the local Universe and their feedback effect on galaxies. *MNRAS* **2019**, *483*, 4586–4614, [arXiv:astro-ph.GA/1805.05352]. <https://doi.org/10.1093/mnras/sty3449>.
16. Gallerani, S.; Pallottini, A.; Feruglio, C.; Ferrara, A.; Maiolino, R.; Vallini, L.; Riechers, D.A.; Pavesi, R. ALMA suggests outflows in $z \sim 5.5$ galaxies. *MNRAS* **2018**, *473*, 1909–1917, [arXiv:astro-ph.GA/1604.05714]. <https://doi.org/10.1093/mnras/stx2458>.
17. Heckman, T.M.; Alexandroff, R.M.; Borthakur, S.; Overzier, R.; Leitherer, C. The Systematic Properties of the Warm Phase of Starburst-Driven Galactic Winds. *ApJ* **2015**, *809*, 147, [arXiv:astro-ph.GA/1507.05622]. <https://doi.org/10.1088/0004-637X/809/2/147>.
18. Manzano-King, C.M.; Canalizo, G.; Sales, L.V. AGN-Driven Outflows in Dwarf Galaxies. *ApJ* **2019**, *884*, 54, [arXiv:astro-ph.GA/1905.09287]. <https://doi.org/10.3847/1538-4357/ab4197>.

Disclaimer/Publisher’s Note: The statements, opinions and data contained in all publications are solely those of the individual author(s) and contributor(s) and not of MDPI and/or the editor(s). MDPI and/or the editor(s) disclaim responsibility for any injury to people or property resulting from any ideas, methods, instructions or products referred to in the content.